SMJ Singapore Medical Journal



# Detectability of feeding arteries using automated feeding artery detection software based on CT arteriography in transarterial embolisation


Takatoshi Kubo[1,2], MD, PhD, Yasuaki Arai[2], MD, PhD, Miyuki Sone[2], MD, PhD, Takatsugu Magara[2], MS, Shunsuke Sugawara[2], MD, PhD, Masahiko Kusumoto[2], MD, PhD, Osamu Abe[1], MD, PhD

[1]Department of Radiology, the University of Tokyo Hospital, [2]Department of Diagnostic Radiology, National Cancer Center Hospital, Tokyo, Japan

**Correspondence:** Dr Takatoshi Kubo, Assistant Professor, Department of Radiology, the University of Tokyo Hospital, 7-3-1 Hongo, Bunkyo-ku, Tokyo 113-8655, Japan. kubo.tky@gmail.com



**Singapore Med J 2022, 1–11**
**https://doi.org/10.11622/smedj.2022060**
Published ahead of print: 25 May 2022

## INTRODUCTION

To achieve transarterial embolisation (TAE) effectively and safely, accurate selective embolisation of feeding arteries is important. However, identification of feeding arteries in TAE is sometimes difficult and requires multiple selective digital subtraction angiography (DSA) and/or computed tomography arteriography (CTA) or cone beam computed tomography arteriography (CBCTA) procedures.

Automated feeding artery detection (AFD) software using CTA or CBCTA has become available for the identification of feeding arteries. A high detectability of feeding arteries has been reported for the AFD software in transcatheter arterial chemoembolisation (TACE) for liver tumours.[1-5] In general, once AFD software analyses non-selective CTA/CBCTA, it automatically and rapidly identifies feeding arteries and allows them to be visualised as volume rendered images and/or as multiplanar reconstruction images. Because of the high rate of feeding artery detection and the usability of AFD, it has been used as an intraoperative navigation software in a wide variety of TAE cases in clinical practice.

All previous reports of AFD software have been based on CBCTA (AFD-CBCTA).[1-8] Despite the proven value of AFD-CBCTA, it is limited by the requirement for a software-compatible CBCT system, a small field of view, and a reduced signal-to-noise ratio of CBCT itself. Recently, AFD based on CTA (AFD-CTA) has emerged as a new form of AFD software that might eliminate the drawbacks of CBCTA-AFD. However, there have been no reports on the detectability of feeding arteries using commercially available AFD-CTA.

The purpose of this study was to evaluate the rate of feeding artery identification by AFD-CTA for TAE of renal tumours before cryoablation.

## METHODS

This retrospective study was conducted with the approval from the institutional review board. Informed consent was waived in view of the retrospective study design.

A total of 24 patients who underwent preoperative TAE before cryoablation of a primary renal tumour, and both DSA and CTA from the main renal artery between April 1, 2018 and March 31, 2019 were evaluated. The patients' characteristics are shown in Table I. The mean tumour size was 22.3 mm (SD 6.9, range 12–37), and all tumours were classified as T1a; the average radius exophytic/endophytic nearness anterior/posterior location (RENAL) nephrometry score[9] was 9.1 (SD 1.2, range 7–12). Percutaneous needle biopsy was performed in all patients, and 91.6% (22/24) were pathologically diagnosed with renal cell carcinoma. The remaining two cases were initially suspected to be renal cell carcinoma and underwent TAE and cryoablation but were ultimately diagnosed as benign lesions.

**Table I: Characteristics of the study patients.**

| Characteristics | Value |
|---|---|
| Mean age (y) | 70.9 ± 11.1 (43–88) |
| Sex | |
| Male | 19 |
| Female | 5 |
| Tumour pathology | |
| Renal cell carcinoma | 22 |
| Benign | 2 |
| Mean tumour size (mm) | 22.3 ± 6.9 (12–37) |
| Radius exophytic/endophytic nearness anterior/posterior location (RENAL) nephrometry score | 9.1 ± 1.2 (7–12) |
| Mean number of feeding arteries | 1.4 ± 0.7 (1-3) |
| Tumour visibility on DSA from the main renal artery | |
| Clear | 17 |
| Unclear | 7 |

*Values in parentheses represent ranges. DSA: digital subtraction angiography*

A 3 to 5-F catheter was advanced to the main renal artery. In all cases, CTA was performed at first. CTA was performed using an Angio-CT system (INFX-8000C/ Aquilion 16;

Canon Medical Systems, Ohtawara, Japan) with a contrast agent (Oypalomin 300; Fuji Pharma Co., Ltd, Tokyo, Japan) injected at 2 mL/s for 6 s, and images were acquired immediately after the injection (tube voltage: 120 kV, tube current: the automatic tube current modulation system (volume EC), field of view: 320–450 mm, slice thickness: 1 mm, reconstruction kernel: FC 15). After CTA, DSA was performed by injecting the contrast agent (Oypalomin 300; Fuji Pharma Co., Ltd, Tokyo, Japan) at approximately 3 mL/s for about 3 s, and the frontal images were acquired at 4.5 frames/s.

With reference to the CTA and DSA images, a microcatheter (1.7-F Progreatλ17; Terumo, Tokyo, Japan, or 1.9-F Asahi Tellus C3; Asahi Intecc, Nagoya, Japan) was inserted into a vessel regarded as a feeding artery, and the contrast medium was injected via the microcatheter to confirm whether the tumour was observed on fluoroscopy, DSA, or CTA. When the artery was confirmed as the feeding artery, the embolisation was performed. When the enhancement of tumour was not confirmed with contrast injection, a microcatheter was inserted into another vessel regarded as a feeding artery, and the same procedure was repeated.

Embolisation of feeding arteries was performed with iodised oil (Lipiodol; Andre Guerbet, Aulnay-sous-Bois, France) and hand-cut gelatin sponge particles (Serescue; Nippon Kayaku, Tokyo, Japan). Embolisation was terminated when the deposition of iodised oil in the tumour was confirmed with sufficient certainty by fluoroscopy or CT.

The analysis of feeding arteries was retrospectively performed by AFD-CTA (Embolisation Plan; Canon Medical Systems, Ohtawara, Japan) using CTA images acquired from the main renal artery. First, the tumour was marked using the segmentation function on the CTA image on the software. Next, the virtual catheter tip position was marked on the CTA image on the software. The software then automatically identified potential arteries feeding the tumour and visualised them on the automatically generated volume rendering and multiplanar reconstruction images. The analysis of the feeding arteries took approximately 30 s or less, and

a total of about 2 min before the feeding arteries were visualised with AFD-CTA.

Using DSA images from the main stem of the renal artery, feeding arteries were retrospectively determined based on the consensus of two board-certified radiologists.

Arteries that showed iodised oil deposition on fluoroscopy or CT after selective embolisation with iodised oil were regarded as feeding arteries. The identification rates of feeding arteries by AFD-CTA and DSA were compared. The identification rate was further evaluated by dividing the tumours into two groups: one of tumours with distinct tumour enhancement, and a second group of tumours without distinct tumour enhancement on the DSA.

JMP® Pro version 14.0.0 (SAS Institute, Cary, NC, USA) was used for the statistical analysis. The Fisher's accuracy test with a significance level of less than 5% was used.

**RESULTS**

The results are summarised in Table II. In total, 34 feeding arteries were eventually embolised. Iodised oil deposition on tumours was observed in all cases; therefore, the feeding arteries were accurately identified through embolisation, although additional feeding arteries may have been present.

**Table II: Identification of feeding arteries.**

| Tumour characteristics and methods | No. of identified feeding arteries (%) | p-value |
|---|---|---|
| All tumours | 34 | |
| DSA | 14 (41.2%) | < 0.0001 |
| AFD-CTA | 34 (100%) | |
| Tumours with distinct enhancement on DSA from the main renal artery | 26 | |
| DSA | 14 (53.8%) | < 0.0001 |
| AFD-CTA | 26 (100%) | |
| Tumours with indistinct enhancement on DSA from the main renal artery | 8 | |
| DSA | 0 (0%) | < 0.0001 |
| AFD-CTA | 8 (100%) | |

*AFD-CTA: automated feeding artery detection software based on computed tomography arteriography; DSA: digital subtraction angiography*

The identification rate of feeding arteries was 100% (34/34) on AFD-CTA, which was significantly higher than the rate achieved with DSA [41.2% (14/34); $p<0.0001$]. In 17 tumours with distinct tumour enhancement on DSA, 26 arteries from the corresponding main renal artery were confirmed as feeding arteries. The identification rate was 100% (26/26) on AFD-CTA and significantly lower at 53.8% (12/26) on DSA ($p<0.0001$). Further, in seven tumours without distinct tumour enhancement on DSA, 8 arteries from the corresponding main renal artery were confirmed as feeding arteries, and the identification rate was 100% (8/8) on AFD-CTA and 0% (0/8) on DSA ($p<0.0001$) (Fig. 1).

A total of 49 vessels were identified as potential feeding arteries using AFD-CTA. Of these, 35 received selective injection of contrast via microcatheters, and one was not a feeding artery. In the remaining 14 of the identified vessels, selective injection of contrast was not performed. In contrast, 24 vessels were identified as potential feeding arteries on DSA. Of these, 19 received selective injection of contrast via microcatheters, and five were not feeding arteries. In the remaining five of the identified vessels, selective injection of contrast was not performed.

## DISCUSSION

In the present study, AFD-CTA from the main renal artery showed a significantly higher identification rate of feeding arteries compared with DSA from the main renal artery in patients who received TAE of renal tumours before cryoablation.

This is the first report on the detectability of feeding arteries using AFD-CTA. This study confined the target to TAE of renal tumours before cryoablation. TAE of renal tumours before cryoablation has been reported to be an effective therapeutic strategy to prevent post-procedural bleeding and to visualise tumours with lipiodol accumulation.[10,11] However, due to the complexity of the renal vascular anatomy, identification of feeding arteries in TAE of

renal tumours is sometimes difficult with conventional methods such as DSA and CTA. According to the result of the present study, AFD-CTA might be useful in such cases.

The detectability of feeding arteries with AFD-CTA in the present study was similar to that reported for AFD-CBCTA in previous studies.[1-5] Our results suggest that AFD-CTA and AFD-CBCTA are similar in their abilities to detect feeding arteries, although the target organs and diseases differ. Therefore, AFD-CTA may be also useful in TACE and other TAE procedures, for which favourable results have already been reported for AFD-CBCTA.[1-6,8] Further studies are needed to assess the usefulness of AFD-CTA in these procedures.

AFD-CTA is considered to have an advantage over AFD-CBCTA in terms of versatility. AFD-CBCTA requires a software-compatible CBCT system, which may represent a major obstacle because of operational requirements. In contrast, AFD-CTA can be used to analyse feeding arteries using any type of CT images, regardless of the system. In this study, angio-CT, in which the fluoroscopy system and CT are integrated, was used to obtain CTA images, but the CT system itself was a conventional diagnostic CT system. It is, therefore, possible to analyse feeding arteries in the same way, by transporting patients to the CT room after the catheter insertion is performed in an angiographic room, and acquiring CTA scans using diagnostic CT, as has been reported in the liver.[12,13] However, in institutions that do not have Angio-CT systems, the AFD-CTA might be recommended for limited cases in which the feeding arteries cannot be easily identified only by the DSA images because transporting the patients to the CT room might take time.

In this study, the detectability of feeding arteries with pre-embolisation imaging such as intravenous CT angiography could not be assessed due to the nature of a retrospective study. The analysis of pre-embolisation imaging might improve the detectability of feeding arteries without AFD-CTA. Further studies are needed to compare AFD-CTA to pre-embolisation imaging.

This study was based on retrospectively analysed data acquired during the TAE procedure. In addition, the potential feeding arteries identified by AFD-CTA and DSA (14 and 5 arteries, respectively) were not evaluated during the procedure. It is unclear whether these unassessed arteries were indeed feeding arteries. Therefore, the accuracy of the AFD-CTA and DSA for detecting the feeding arteries might be overestimated. Further prospective studies evaluating all identified potential feeding arteries are needed in this regard.

There are other limitations to this study. First, it was a retrospective study with a small number of patients. Further prospective studies are needed to evaluate intraoperative detectability of feeding arteries by AFD-CTA. Second, the target population was limited to patients with renal tumours that underwent TAE prior to cryoablation. DSA alone may have sufficient capability to identify feeding arteries in other tumours, such as large tumours and angiomyolipomas that are not indicated for cryoablation. In contrast, the volume of injected contrast medium was lower on DSA than on CTA, which might have reduced the detectability of feeding arteries on DSA. In addition, not all feeding arteries were embolised in the present study because embolisation was terminated when sufficient iodised oil had been deposited for cryoablation. Therefore, there may be other potential feeding arteries that have not been assessed, and thus the ability to identify feeding arteries may have been overestimated.

In conclusion, AFD-CTA is effective as a method to identify feeding arteries in TAE for renal tumours before cryoablation. AFD-CTA may also be applied to identify feeding arteries in other procedures such as TACE.

## ACKNOWLEDGEMENTS

We would like to thank Editage (www.editage.com) for English language editing. This study was funded by the National Cancer Center Research and Development Fund (29-A-11). This study was conducted with the approval from the institutional review board. Informed consent

was waived in view of the retrospective study design.

## CONFLICT OF INTEREST

Dr Kubo reports personal fees from Canon Medical Systems, outside the submitted work. Dr Arai reports personal fees from Canon Medical Systems, outside the submitted work. Dr Sone reports grants and non-financial support from Canon Medical Systems, during the conduct of the study; personal fees from Canon Medical Systems, outside the submitted work. Dr Sugawara reports personal fees from Canon Medical Systems, outside the submitted work. Dr Abe reports grants from Canon Medical Systems, personal fees from Canon Medical Systems, outside the submitted work. The other authors have nothing to disclose.

## REFERENCES

1. Miyayama S, Yamashiro M, Hashimoto M, et al. Identification of small hepatocellular carcinoma and tumor-feeding branches with cone-beam CT guidance technology during transcatheter arterial chemoembolization. J Vasc Interv Radiol 2013; 24:501-8.
2. Miyayama S, Yamashiro M, Ikuno M, Okumura K, Yoshida M. Ultraselective transcatheter arterial chemoembolization for small hepatocellular carcinoma guided by automated tumor-feeders detection software: technical success and short-term tumor response. Abdom Imaging 2014; 39:645-56.
3. Miyayama S, Yamashiro M, Nagai K, et al. Efficacy of automated tumor-feeder detection software using cone-beam computed tomography technology in transarterial embolization through extrahepatic collateral vessels for malignant hepatic tumors. Hepatol Res 2016; 46:166-73.

4. Chiaradia M, Izamis ML, Radaelli A, et al. Sensitivity and reproducibility of automated feeding artery detection software during transarterial chemoembolization of hepatocellular carcinoma. J Vasc Interv Radiol 2018; 29:425-31.
5. Joo SM, Kim YP, Yum TJ, et al. Optimized performance of FlightPlan during chemoembolization for hepatocellular carcinoma: importance of the proportion of segmented tumor area. Korean J Radiol 2016; 17:771-8.
6. Miyayama S, Yamashiro M, Sugimori N, et al. Outcomes of patients with hepatocellular carcinoma treated with conventional transarterial chemoembolization using guidance software. J Vasc Interv Radiol 2019; 30:10-8.
7. Iwazawa J, Ohue S, Hashimoto N, Takashi M. Comparison of the number of image acquisitions and procedural time required for transarterial chemoembolization of hepatocellular carcinoma with and without tumor-feeder detection software. Radiol Res Pract 2013; 2013:580839.
8. Miyayama S, Yamashiro M, Nagai K, et al. Usefulness of dual-phase cone-beam computed tomography during arteriography and automated tumour-feeder detection software in transarterial embolization for obscure arterial bleeding in the abdomen. J Med Imaging Radiat Oncol 2018; 62:364-9.
9. Kutikov A1, Uzzo RG. The R.E.N.A.L. nephrometry score: a comprehensive standardized system for quantitating renal tumor size, location and depth. J Urol 2009; 182:844-53.
10. Gunn AJ, Mullenbach BJ, Poundstone MM, et al. Trans-arterial embolization of renal cell carcinoma prior to percutaneous ablation: technical aspects, institutional experience, and brief review of the literature. Curr Urol 2018; 12:43-9.
11. Kajiwara K, Yoshimatsu R, Nishimori M, et al. Efficacy of arterial infusion of iodized oil on CT-guided cryoablation for renal cell carcinoma. Minim Invasive Ther Allied Technol 2020 Mar 5. https://doi.org/10.1080/13645706.2020.1734622. [Epub ahead of print]

12. Hayashi M, Matsui O, Ueda K, et al. Correlation between the blood supply and grade of malignancy of hepatocellular nodules associated with liver cirrhosis: evaluation by CT during intraarterial injection of contrast medium. AJR Am J Roentgenol 1999; 172:969-76.
13. Hayashi M, Matsui O, Ueda K, et al. Progression to hypervascular hepatocellular carcinoma: correlation with intranodular blood supply evaluated with CT during intraarterial injection of contrast material. Radiology 2002; 225:143-9.

**FIGURE**

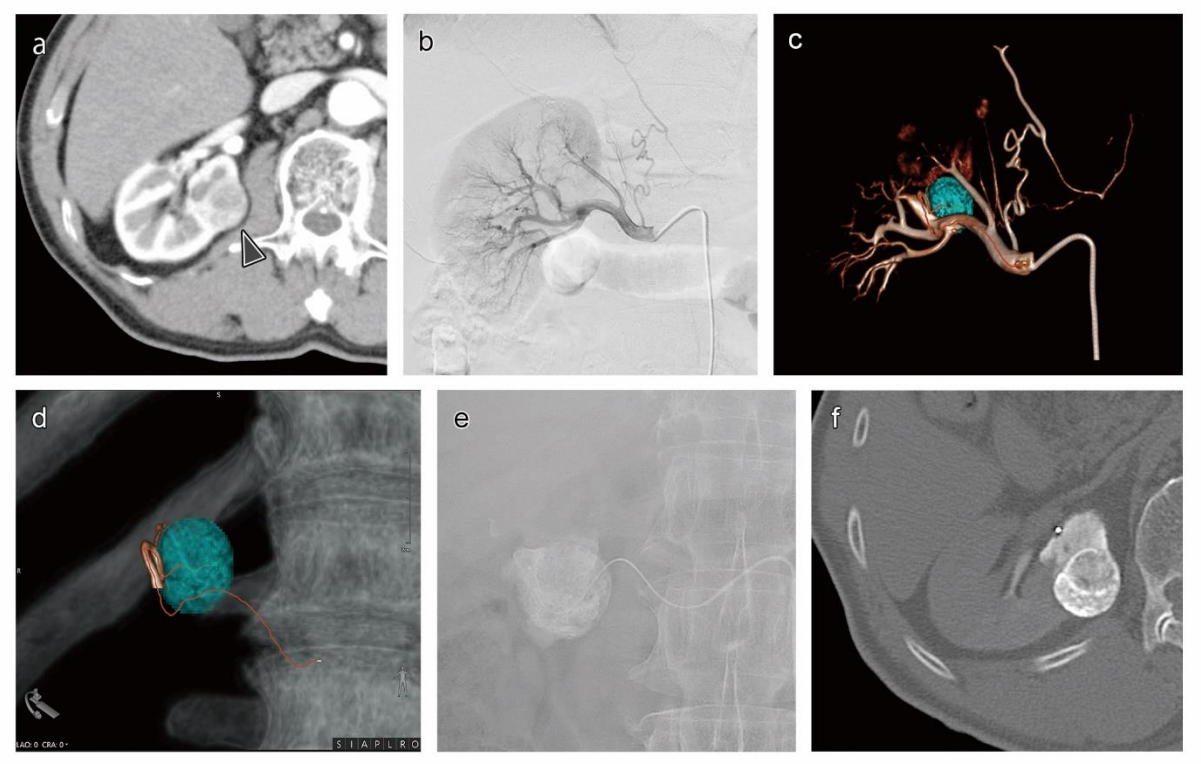


**Fig. 1** A case of feeding artery not identifiable with DSA but identifiable with AFD-CTA. **(a)** Contrast enhanced CT revealed a 25 mm renal cell carcinoma in the middle portion of the right kidney (arrowhead). **(b)** DSA from the right renal artery could not reveal the tumour and feeding arteries. **(c), (d)** AFD-CTA from the right renal artery identified the feeding artery as a red line. **(e)** The identified feeding artery was selected and embolised. **(f)** CT immediately after TAE showed a clear deposition of iodised oil in the tumour. CT: computed tomography; AFD-CTA: automated feeding artery detection software based on computed tomography arteriography; DSA: digital subtraction angiography; TAE: transarterial emboliation.